The research of optical windows used in aircraft sensor systems

Zhou Feng(周 峰), Li Yan(李 岩)†, and Tang Tian-Jin(汤天瑾)

Beijing Institute of Space Mechanics & Electricity, Beijing 100076, *China*

(Received 28 August 2011; revised manuscript received 15 September 2011)

The optical windows used in aircrafts protect their imaging sensors from environmental effects. Considering the imaging performance, flat surfaces are traditionally used in the design of optical windows. For aircrafts operating at high speeds, the optical windows should be relatively aerodynamic, but a flat optical window may introduce unacceptably high drag to the airframes. The linear scanning infrared sensors used in aircrafts with, respectively, a flat window, a spherical window and a toric window in front of the aircraft sensors are designed and compared. Simulation results show that the optical design using a toric surface has the integrated advantages of field of regard, aerodynamic drag, narcissus effect, and imaging performance, so the optical window with a toric surface is demonstrated to be suited for this application.

Keywords: optical window, aircraft sensor, narcissus effect, toric surface

PACS: 42.15.Dp, 42.15.Eq, 42.15.Fr **DOI:** 10.1088/1674-1056/21/6/064201

1. Introduction

The optical windows are the most crucial optical components of the electro-optical (EO) imaging sensors used in aircraft systems. Behind each window there is an imaging sensor system which views the scene through the optical window. The window must be transparent to the radiation of the operating wavelength of the sensor and resist attack from external forces.[1]

This paper deals with an imaging sensor that moves via a pivoting motion to complete IR line scanning over a wide angular range, as seen in Fig. 1. Three kinds of windows are designed and several performances are compared in order to choose an optimal optical window among them for this application.

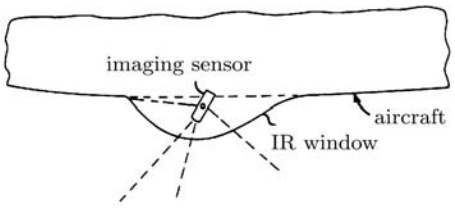


Fig. 1. Imaging sensor scanning a field of regard behind the IR window.

The operating wavelength is in a range of 8 μm–11.5 μm for IR search and tracking, which is working by linear scanning in one dimension across a –20°–20° field of regard (FOR), the other dimension has a –0.5°–0.5° field of view (FOV).

2. Aerodynamic drag concept

The previous technique used for aircraft windows required the use of flat sections. This requirement stemmed from the fact that the technique used in manufacturing windows only allowed flat surfaces. Aircraft windows sometimes use several segments to allow wide fields of regard for the imaging optical systems (see Fig. 2). There are obvious disadvantages associated with using these traditional shapes. Aircraft windows composed of one or several flat segments can cause turbulence and increase drag. Also, the radar cross section (RCS) is adversely affected.

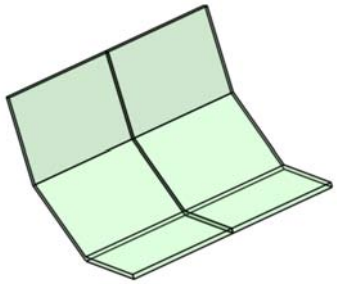


Fig. 2. (colour online) Aircraft windows composed of several segments.

†Corresponding author. E-mail: ppmmliyan@yahoo.com.cn

© 2012 Chinese Physical Society and IOP Publishing Ltd

It is better that the optical windows use a non-flat shape and conform to other requirements of the airframe, such as drag, control of turbulence, RCS, and high-resolution, wide field of regard imaging. Figure 3 shows how the optical window has changed from a flat window to a non-flat optical surface.[2]

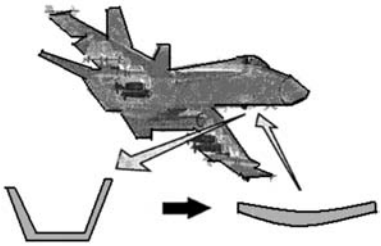


Fig. 3. Replacement of traditional windows to enhance system performance.

3. Narcissus performance of the IR window

The narcissus analysis is intended to be used with an IR system that has an internal scanner and will be used with a cooled detector. These types of systems are subject to a peculiar type of defect in the imagery caused by single surface retro-reflections. The system designed in this paper comprises an IR window, imaging lenses, a cold stop, a focal plane array (FPA), and so on. In a simulation model, both a source and a receiver are set on the FPA and only the surfaces of the optical window are set to have reflectance for analysing the narcissus effect of the window surfaces. Figure 4 shows the simulation model. Tracing the rays emitted from the image surface, we can obtain the distribution of energy on the receiver which can represent the narcissus effect caused by the optical window surfaces.[3]

Different optical window surface types may cause different narcissus effects. Three kinds of optical systems including windows with a flat surface, a spherical surface, and a Y-toroid surface are designed, respectively. The designs are for use with a linear scanner at X-dimension across the –20°–20° FOR, the field of view of the Y-dimension is –0.5°–0.5°, and the aperture of the system is 80 mm.



Fig. 4. (colour online) Model used for simulation of the narcissus effect.

In order to simulate the effect of narcissus, a Lambertian surface source is located at the position of the detector. The layout of the ray tracing of the system with a flat window is shown in Fig. 5. The rays emit from the detector, and are retro-reflected by the window surface back to the detector surface because the surfaces of the flat window are normal to the optical axis. The narcissus effect of the window with a spherical surface and the Y-toroid surface are also simulated, which are shown in Fig. 6. The irradiance of the narcissus energy on the receiver, caused by the flat IR window, exceeds those by the spherical window and toric window greatly. The Y radius of the above spherical surface is optimized to be 1600 mm, and the Y radius of the Y-toroid surface is 2500 mm.

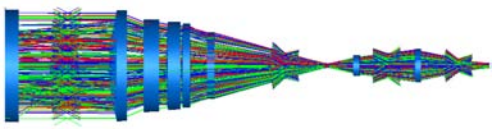
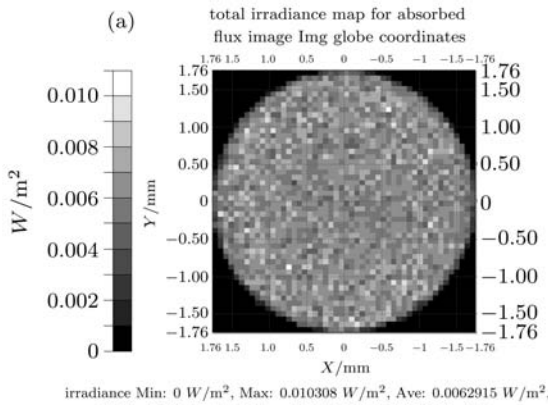
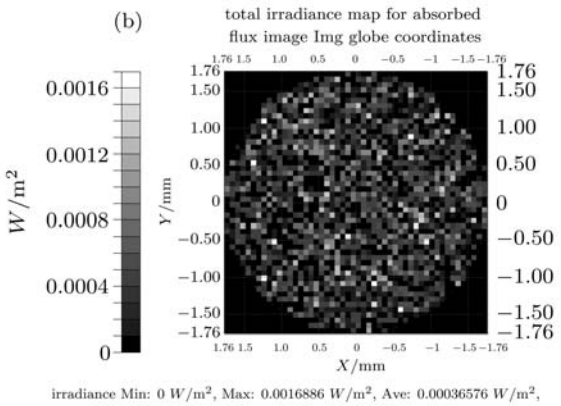


Fig. 5. (colour online) The ray tracing layout for simulation of the narcissus effect.





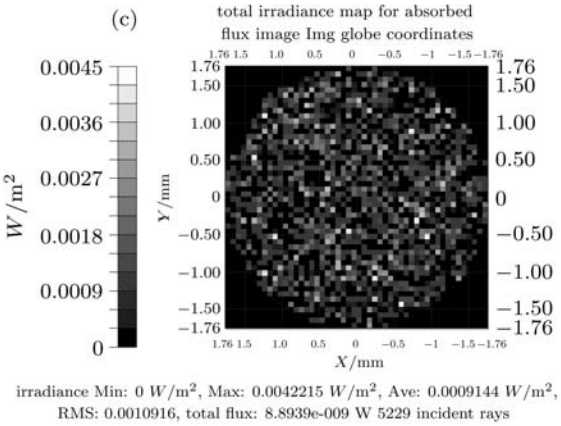


Fig. 6. Distributions of energy on the receiver: (a) flat window, (b) spherical window, (c) toric window.

4. Comparison of the imaging performances of the IR windows

The sagittal layout of the optical system with a flat surface after optimization is shown in Fig. 7. The first element is the germanium window, and the imaging sensor behind it scans the X field by the gimbal located in front of the second optical element. From the modulation transfer function (MTF) of the system across the full FOR shown in Fig. 8, we can see the imaging performance of the optical system with flat window remains good.

Figure 9 shows the MTF of the system with a spherical IR window across the full FOR. The outer surface of the germanium window is now a spherical shape with a Y radius of 1600 mm after optimization. The imaging performance of the 0° FOR is good, but that at the edge of the FOR is worse. When the sensor scans across the full FOR behind the spherical optical window, the optical system will not be rotationally symmetric. Off-axis aberrations will be introduced and are invariant with the FOR since the optical system loses rotational symmetry.[4]

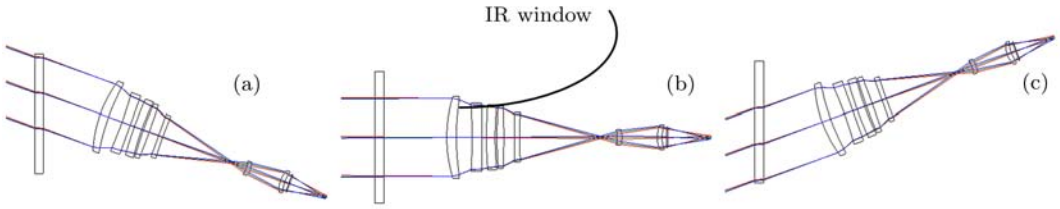


Fig. 7. (colour online) Sagittal layout of the imaging system scan behind a flat window: (a)–20° FOR, (b) 0° FOR, (c) 20° FOR.

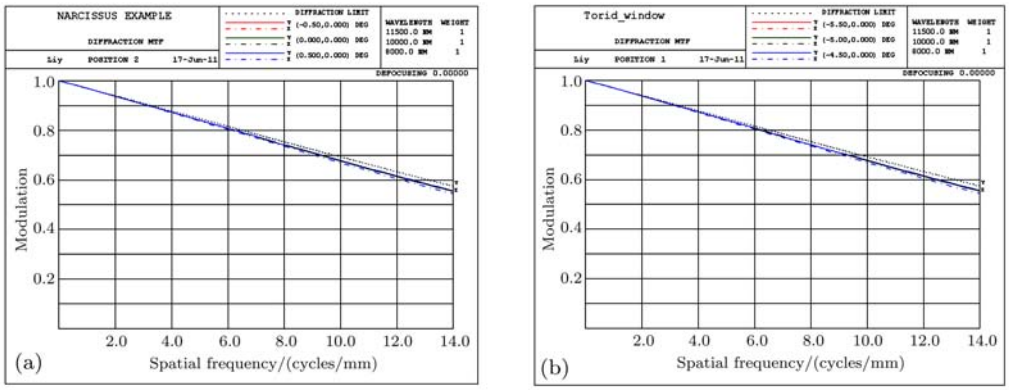


Fig. 8. (colour online) MTF of a flat window: (a) MTF of 0° FOR, (b) MTF of –20° and 20° FOR.

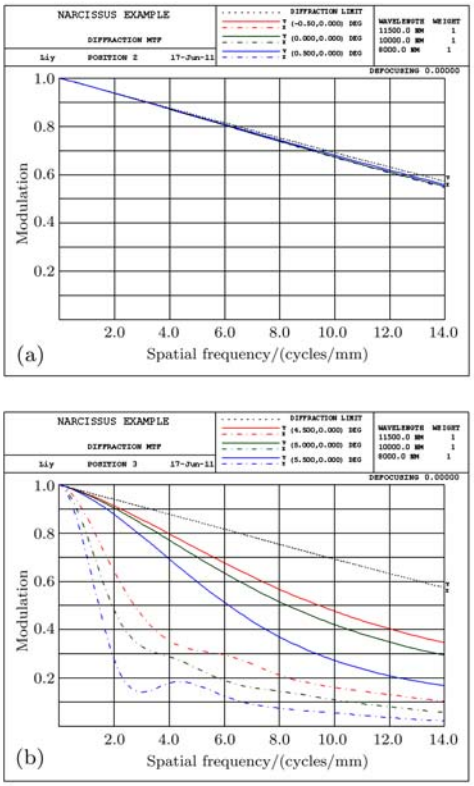


Fig. 9. (colour online) MTF of spherical window: (a) MTF of 0° FOR, (b) MTF of –20° and 20° FOR.

To compensate the dynamic aberrations of the optical system with the spherical window, the outer surface of the germanium window is changed into a Y toroid surface type using Code V software, whose definition in the Y–Z plane is expressed as

$$Z = \frac{\mathrm{CUY}y^2}{1+\mathrm{SQRT}\{1-(k+1)\mathrm{CUY}^2y^2\}} + Ay^4 + By^6 + Cy^8 + \cdots \quad (1)$$

Change surface type into Y-toroidal shape on the selected surface, with aspheric contour in Y–Z plane. A Y-toroidal surface is defined by X radius, Y radius, Conic constant (K), and 4th–10th order coefficients (A, B, C, and D).[5] The X radius is set to be zero in this application, and the outer surface has a cylinder surface with aspheric coefficients in Y–Z plane, so the IR window is equivalent to a flat glass in X–Z plane. When the imaging sensor is scanning across the X field, the IR window with Y-toroidal surface may not induce the dynamic aberration across the full field of regard.

The Y radius of the Y-toroidal surface is optimized to be 1600 mm. In order to make the Y power and X power of this optical system equivalent, an optical corrector with X-toroidal surface is added and located at the third element shown in Fig. 10. The X-toroidal surface type in Code V software defined in the X–Z plane is as indicated in formula (2). The expression of this formula is similar to formula (1). The Y radius is also set to be zero, and the X radius is varied during the automatic optimization in the program.[6]

$$Z = \frac{\mathrm{CUY}x^2}{1+\mathrm{SQRT}\{1-(k+1)\mathrm{CUY}^2x^2\}} + Ax^4 + Bx^6 + Cx^8 + \cdots \quad (2)$$

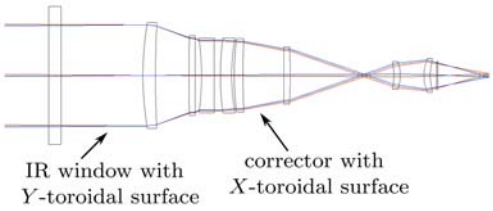


Fig. 10. (colour online) IR window with a Y-toroidal surface using an optical corrector with an X-toroidal surface.

The X radius of this surface in the optical corrector is optimized to be 1202.51 mm. From the MTF of the system across the full FOR as shown in Fig. 11, we

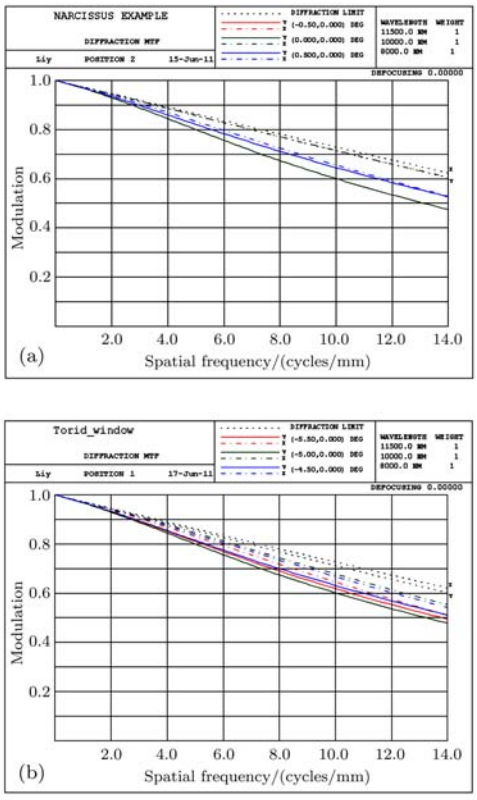


Fig. 11. (colour online) MTFs of toric window: (a) MTF of 0° FOR, (b) MTF of –20° and 20° FOR.

can see that the imaging performance of the optical system with toric window remains good. When the observation area needs to be enlarged, the 4th–10th

order coefficients of the Y-toroidal and X-toroidal surfaces may be changed during the automatic optimization to achieve good imaging performances across the larger full FOR.

5. Summary

The optical design of the IR windows used in aircraft can be considered to be optimal, and is affected by considerations of weapon integrated requirements such as field of regard, aerodynamic drag, narcissus effect, imaging performance, and cost. In this paper IR windows with a toric surface are presented, which is feasible for this application. To make the toric surface of the optical windows realistic, challenges have to be overcome in fabrication and testing.

References

[1] Robert H Au 1990 "Optical Window Systems", *Window and Dome Technologies and Materials* II

[2] Thomas A Mitchell A, Jose M and Sasian B 1999 *Proc. SPIE* **3705** 209

[3] Juan L R and Lan L 1992 *Proc. SPIE* **1752** 325

[4] Li Y, Li L, Huang Y F and Liu J G 2009 *Chin. Phys.* B **18** 565

[5] ORA. CODE V10.2 *Reference Manual* "Defining Y-Toroid Surfaces" pp 4–78

[6] ORA. CODE V10.2 *Reference Manual* "Defining X-Toroid Surfaces" pp 4–75